Water induced chromogenic and fluorogenic signal modulation in a bi-fluorophore appended acyclic amino-receptor system†

Bamaprasad Bag* and Ajoy Pal

Received 9th June 2010, Accepted 15th October 2010
DOI: 10.1039/c0ob00238k

An acyclic amino-receptor based bi-fluorophoric signaling system **3** exhibits water-induced simultaneous dual channel chromogenic and fluorogenic signal modulation. Its micromolar solution in various organic solvents exhibits an enhancement in absorption in the presence of water in trace amounts through the water-induced delactonization of rhodamine dye, rendering a visual perception as a function of colour change. The presence of water molecules also facilitates a fluorescence resonance energy transfer (FRET) from the excited nitro-benz-oxa-diazole fluorophore to rhodamine dye of **3** and leads to an enhancement of emission up to a second order of magnitude. The failure of the reference compounds **2** and **4** to respond under similar conditions reveals the role of structural variation of the receptor on the perturbation of photophysical processes.

Introduction

Chromogenic and fluorogenic signaling probes[1] for detection of analytes of biological, clinical and environmental importance are of immense interest and their recent development is due to various methodological designs, perturbation of photophysical processes involved and optical signal trade-off with analyte concentration. These multi-compartmental miniaturized supramolecular transducers respond to chemical information changes occurring at a receptor unit upon analyte binding by communicating the binding event to a signaling subunit *via* perturbation of operative intercomponent photophysical processes, which results in signal modulation that can be visually perceived and/or instrumentally monitored. A chromogenic signaling module offers naked eye detection of an analyte through a change in colour (or variation in absorption) while fluorescent probes have the advantage of high sensitivity and selectivity, shorter response time, non-complicated sampling, non-destructive and non-evasive properties and thus offer real-time monitoring of the processes occurring at different time scales. Hence, owing to different operation conditions, it is advantageous to design probes that use both chromogenic as well as fluorescence signaling module for detection of the targeted analytes.

The rhodamine based dyes have recently been extensively used for bio-labelling in bio-imaging[2] and in material research[3] because of their excellent spectroscopic properties such as high absorption coefficient, high fluorescence quantum yield, absorption and emission at longer wavelength *etc*. The rhodamine based chromogenic and fluorogenic chemosensors for detection of various analytes such as transition and heavy metal ions,[4–7] carboxylate[8] and hypochlorite[9,10] anions, NO,[11] aminoalcohols,[12] aminoacids[13] *etc.* have been receiving increasing attention due to their capability of modulating absorption and emission signals in aqueous media and thus promise a virtue of practical applications. The design of these chemosensors follows a straightforward protocol:- (a) exploitation of either rhodamine's inherent properties such as high solubility in an aqueous medium or/and (b) their structure–function correlation. The commonly existing spirolactam form of rhodamine is colourless and non-fluorescent in protic solvents, which structurally equilibrates to a colored and highly fluorescent ring-opened amide form upon analyte binding. Several such rhodamine based chemosensors[3b,6,7] for transition and heavy metal ions have been reported to perform sensory activity in aqueous or mixed organic–aqueous medium. The interesting spectral characteristics of rhodamine's structural transformation involving its lactolization–delactonization process still provide ample scope for development of new signaling probes for efficient recognition of analytes of biological and environmental interest. Further, not much work has been focused on development of rhodamine based chemosensors exploiting either their spectroscopic properties as a function of the solvent polarity or even using water as an analyte to a probe rather than as a medium. To the best of our knowledge, no such chemosensor for water where water acts as a guest is available in the literature. Chemosensing probes that exert their signaling activity in the presence of water molecules find a wide range of applications in material based research, particularly those envisaged towards futuristic moisture sensing applications. The manual gravimetric drying moisture determination methods currently employed by most mineral processing plants, which highly rely on a weight-loss method, are time consuming and lack accuracy for automatic control. Molecular probe based moisture sensors provide a parallel and viable solution; such a sensing probe[14] is Fe[2,6-bis-(triazol-3-yl)-pyridine)]$_2$Cl$_2$ complex, which enables the quantitative and qualitative determination of moisture through Mössbauer spectroscopy, relying on a moisture induced change in ground state electronic spin. In this context, design of a chromogenic/fluorogenic probe for water molecules which relies

Colloids and Material Chemistry Department, Institute of Minerals and Materials Technology (CSIR), Bhubaneswar-751013, India. E-mail: bpbag@immt.res.in; Fax: + 91 674 258 1637; Tel: + 91 674 258 16 35

† Electronic supplementary information (ESI) available: ^{1}H-, ^{13}C-NMR, ESI-MS spectra, various absorption and emission spectroscopic data, control experiments and geometrical optimization of the structures of ligands **1**–**4**. See DOI: 10.1039/c0ob00238k

on 'non-evasive, non-destructive and easy to handle' methods to express the sensing event promises to be advantageous.

In an effort towards realization of these objectives, we report the synthesis and signaling pattern of an acyclic amino-receptor based probe (**3**) which exhibits simultaneous dual channel chromogenic and fluorogenic signaling in the presence of water molecules. Derivatization of bis-(chloroethyl)-amine with 4-chloro-7-nitrobenz-2-oxa-1,3-diazole (4-chloro-7-nitro-benzofurazan, NBD) results in **1** (Scheme 1). Its aliphatic nucleophilic substitution reaction with ethylenediamine followed by condensation with rhodamine-B in ethanol and subsequent purification through column chromatography in neutral alumina affords **3**. The μM solution of **3** in solvents like THF, acetone, MeCN, DMF, DMSO *etc.* at very low concentration is colorless; however, it turns pink in colour upon addition of trace amount of water. Simultaneously, its quenched fluorescence in those solvents results in fluorescence enhancement in presence of water through perturbation of fluorescence resonance energy transfer (FRET)[15] process. Systems containing more than one type of fluorophore where the emission spectrum of donor overlaps with the absorption spectrum of the acceptor facilitates a FRET process through excited state energy transfer between the excited donor→acceptor couple. Reports on metal ion induced FRET OFF–ON signaling in rhodamine based[8,16] probes, though few, are available in literature. In order to understand the photophysical behavior of the rhodamine moiety in the system and its subsequent contribution to water-induced signaling modulation, the reference compound **2** was synthesized[17] through condensation of ethylenediamine with rhodamine-B in ethanol. **4** was synthesized through Schiff base condensation of **2** with *iso*-phthalaldehyde in ethanol followed by reduction with $NaBH_4$ in order to investigate the structural and functional role of the donor N-atom attached with the NBD moiety in **3**. The compounds were characterized by ^{1}H-NMR, ^{13}C-NMR and ESI-MS. The characteristic peak near ~66 ppm (9-carbon) in the ^{13}C-NMR spectrum of the compounds in $CDCl_3$ confirms their predominant existence in rhodamine's spirolactam form. In comparison to the signaling pattern of **3** in the presence of water, the absorption and emission spectral behavior of the reference compounds **2** and **4** reveals their inability to respond under similar conditions.

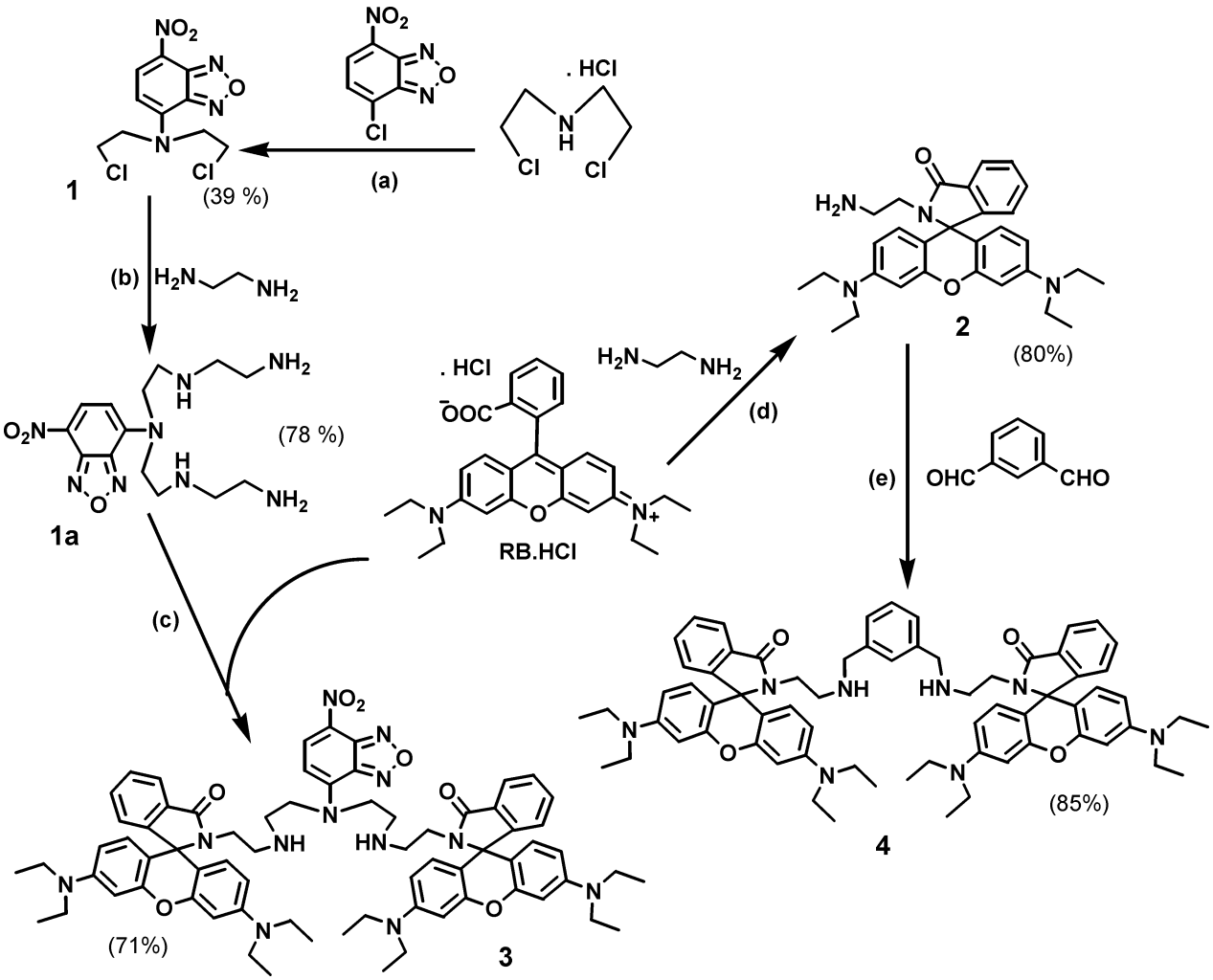

Scheme 1 Schematic representation of synthesis of the ligands (**1–4**). ***Reagent and conditions***: (*a*) K_2CO_3, toluene, reflux, 6 h; (*b*) ethylenediamine, ethanol, K_2CO_3, reflux, 24 h; (*c*) ethanol, reflux, 20 h; (*d*) ethanol, reflux, 16 h; (*e*) ethanol, RT, 24 h, $NaBH_4$.

Results and discussion

UV–vis absorption and emission spectral properties

The absorption transition at ~260–270 nm for all the compounds in various solvents is attributed to the higher energy ligand localized π–π* transition which arises through long-axis parallelism. **1** exhibits two absorption bands at 330–350 nm and 455–473 nm regions, where the lower energy absorption band is attributed to the intramolecular charge transfer (ICT) transition[18,19] from the donor N atom of **1** to the acceptor nitro-group of the NBD moiety which can accept the electron density in its available π symmetry orbitals. As expected, this ICT transition is found to be solvatochromic in nature (λ_{max} = 434 nm in hexane, 41 nm red-shifted in DMSO). The μM solution of **2** absorbs at ~315 nm (ε <30000 dm^3 mol^{-1} cm^{-1}) and does not exhibit any absorption transition at 400–600 nm region and appears colorless. Similarly, **4** also does not absorb in that region in any of these solvents under investigation. This ascertains that the rhodamine exists in its spirolactam conformation in **2** and **4**. On the contrary, the absorption spectral pattern of **3** that incorporates both the chromophores in its architecture is found to be different in various solvents in comparison to the reference compounds **1**, **2** and **4**. The absorption spectra of **3** (conc. 1×10^{-6} M) do not exhibit the characteristic peak corresponding to amino-π-nitro ICT transition of NBD as observed in **1**, instead, a new peak appears at ~550 nm with low molar extinction coefficient (ε <1000 dm^3 mol^{-1} cm^{-1}) in almost all solvents under investigation[20] and their colorless solution ascertains rhodamine's existence in spirolactam form. Although no absorption transition in that region is expected to appear due to the lactonized conformation of rhodamine in **3**, the weak absorption at ~550 nm is probably due to trace of delactonisation[6l] of spiro-ring. The absorption and emission spectra of these compounds are given in Fig. 1.

The reference molecule **1** exhibits a weak solvatochromic emission band at 530 nm in MeCN (494 nm in hexane, 536 nm in DMSO) attributed to a quenched radiative decay of CT excited state due to a photoinduced electron transfer[18,19] (PET) in the form of ICT operative from HOMO of donor *tert*-N atom to its excited nitrobenzofurazan moiety. The semi-empirical molecular orbital calculations of the geometrically optimized structure reveals that the electron density of the highest occupied molecular orbital (HOMO) is localized over the donor amino-group while it drifted away towards acceptor and π-conjugated part in the lowest unoccupied molecular orbital (LUMO), indicative of its ICT nature. The PET-induced low fluorescence quantum yield (ϕ_F) is significantly lower in polar solvents in comparison to that in non-polar solvents, which is due to polarity induced charge–dipole and H-bonding interactions leading towards a considerably faster PET process. On the other hand, the emission spectral pattern of **2** upon excitation at ~500 nm also show a quenched fluorescence centered at ~550 nm due to combined factors:- (a) rhodamine's existence in the spirolactam form which facilitates an efficient intersystem crossing and (b) an operative PET from distal amino group. Similarly **4**, which contains two rhodamine units in its architecture, also exhibits a quenched emission at 625 nm in MeCN upon excitation at 500 nm. The ~75 nm red-shift of the emission maxima of **4** in comparison to that of **2** is assigned to be an excimer formation in **4** as it disappears in lower concentration of the solution. On the contrary, **3** does not fluoresce when excited at 350–450 nm, however, it exhibits a weak solvatochromic emission in the 570–630 nm region upon excitation at 550 nm which is predictably supported by emission pattern of the reference compounds. Further, the HOMO–LUMO electron density map as approximated through semi-empirical calculations reveals that when excited at 350–450 nm, the primary PET process operative from donor N-atom to the acceptor nitro-group of NBD

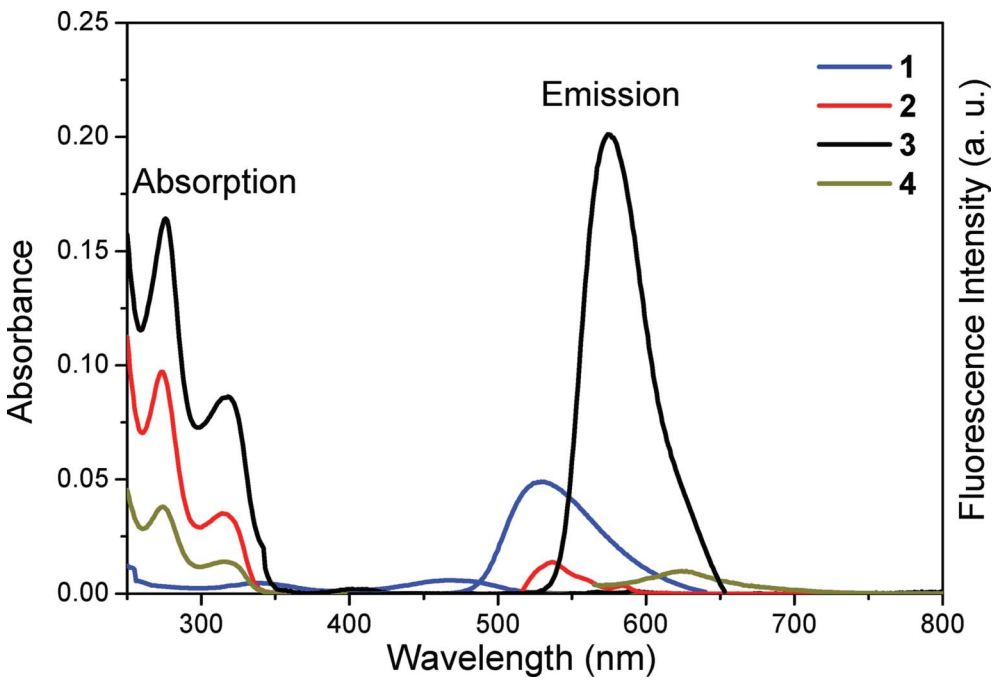

Fig. 1 Absorption and emission spectra of **1–4** (MeCN, conc. 1×10^{-6}M, $\lambda_{ex}^{(1)}$ = 350 nm, $\lambda_{ex}^{(2)}$ = 500 nm, $\lambda_{ex}^{(3)}$ = 350 nm, $\lambda_{ex}^{(4)}$ = 350 nm).

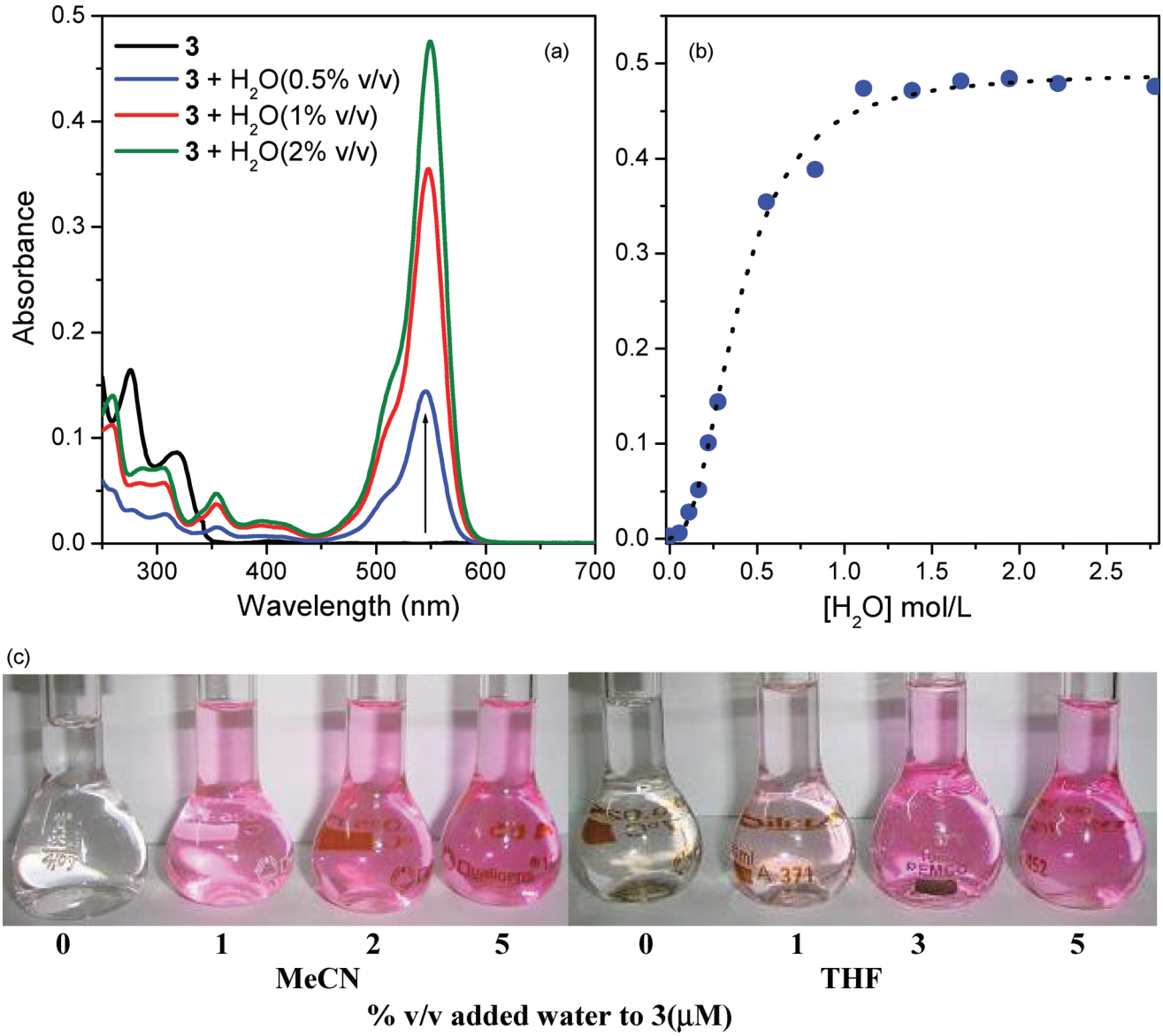

Fig. 2 (a) Absorption spectral pattern of **3** alone (MeCN, 1×10^{-6} M concentration) and in the presence of added H_2O in 0.5%, 1% and 2% v/v. (b) Plot of absorbance of **3** as a function of molar concentration of added water (mol L^{-1}). (c) Change in colour upon addition of water (% v/v) to 3 (μM) in MeCN–THF.

moiety in the form of ICT is responsible for the quenched emission of **3**, not the PET from the amino-donor atom to the rhodamine π-acceptor.[18,19,21] Precisely, the quenched emission of **3** in the longer wavelength region when excited at 450 nm is due to combined contributions of various influential parameters:- (a) the operative PET from amino N-atom to excited NBD fluorophore, (b) the spiro-conformation of rhodamine and (c) the secondary PET from distal N_{amino}- donor atoms to the fluorophores. Of course, some other processes such as internal bond rotation, modulation of non-radiative processes through conformational variation and solvent interactions, and competition between simultaneously operative processes *etc.* may also be involved. As expected, the emission quantum yields (ϕ_F) of all these compounds vary with solvent polarity function.

Absorption spectral pattern in the presence of water

μM colorless solutions of **3** in a few water miscible solvents such as THF, MeCN, acetone, DMF, and DMSO were taken to investigate the effect of water addition on absorption in the visible wavelength region (450–650 nm window). Upon addition of water in various proportions, absorption of **3** in these organic solvents shows a strong enhancement in absorbance at ~550 nm with the appearance of a shoulder at ~515 nm (Fig. 2a) and subsequently its colourless solution turns pink, which is attributed to the water-induced structural transformation of rhodamine's initial spirolactam form to the ring-opened amide form. Further, an absorption peak at 354 nm (in MeCN, logε <4.69) appears upon titration of **3** with water, which is attributed[22] to the associated

Table 1 Absorption and emission spectral data of **1–3** alone and in the presence of H_2O (in % v/v)[a] in various solvents

			Absorption		Emission	
Probes	Solvent	H_2O (%)	log ε	EF	ϕ_F	EF
3	THF	—	2.97	—	0.009	—
		1	4.43	28.9	0.144	16.2
		3	5.54	376.4	0.525	58.3
		5	5.64	467.7	0.541	60.1
	MeCN	—	3.25	—	0.005	—
		1	5.53	190.6	0.295	59.0
		3	5.63	239.9	0.372	74.4
		5	5.68	269.2	0.391	78.2
	Acetone	—	3.76	—	0.013	—
		1	4.60	6.9	0.179	13.8
		3	5.58	66.1	0.224	17.2
		5	5.64	75.9	0.243	18.7
	DMF	—	2.97	—	0.002	—
		1	4.49	33.1	0.031	15.5
		3	5.55	380.2	0.045	22.6
		5	5.65	478.6	0.048	24.0
	DMSO	—	2.97	—	0.002	—
		1	4.48	32.3	0.033	16.5
		3	5.60	426.5	0.049	24.5
		5	5.63	457.1	0.051	25.5
1	MeCN	—	3.79	—	0.001	—
		10	3.93	1.4	< 0.001	< 1
		30	4.04	1.7	< 0.001	< 1
		50	4.04	1.7	< 0.001	< 1
2	MeCN	—	1.30	—	0.007	—
		10	1.30	1	< 0.001	< 1
		30	1.41	1.3	< 0.001	< 1
		50	1.45	1.4	< 0.001	< 1
4	MeCN	—	2.34	—	< 0.001	—
		10	2.34	~ 1	< 0.001	< 1
		30	2.38	~ 1	< 0.001	< 1
		50	2.36	~ 1	< 0.001	< 1

[a] Absorption spectra were taken in 1×10^{-6} M concentration. Emission experimental conditions: concentration of free ligand: $1 \times 10^{-6}/1 \times 10^{-8}$ M; added water in % of v/v with respective solvent; λ_{ex} = 450 nm; excitation and emission band-pass: 5 nm; T = 298 K; The error in ϕ_F is within 10%. EF: Enhancement Factor in comparison to ligand in pure solvent.

$\pi \rightarrow \pi^*$ transition of amino-NBD segment and also observed with **1** under similar conditions. The plot of absorbance as a function of added water to the μM solution of **3** in MeCN reveals that the intensity of the absorption peak enhances gradually up to addition of 2% v/v H_2O (1.11 moles per litre) and remains almost constant even upon further addition (Fig. 2b). The extent of increase in absorption upon water addition is found to be as high as ~500 fold in THF, DMF and DMSO whereas that in acetone resulted in only one order higher in magnitude (Table 1). As the addition of trace amount of water leads to a change in the color of the solution from colorless to pink (Fig. 1c), the probe **3** can be employed for naked-eye detection of water molecules present in various organic solvents. The pink colour development upon addition of water to the MeCN solution at 1×10^{-6}M concentration has a detection limit of 0.3% v/v water added, which can be observed through the naked eye. The water-induced increase in molar absorptivity in the visible region and subsequent colour change as in **3** could not be appreciably observed for **1**, **2** and **4**, neither under similar conditions, nor even at higher probe/guest concentrations. This indicates that the water mediated delactonization of spiro-ring (as in **3**) does not occur in these compounds. The ^{13}C-NMR data in D_2O provides vital information on the ring opening process occurring in **3**. The characteristic chemical shift of tetra-carbon of **3** in the spiro-form at 65.8 ppm disappears in D_2O and moves to the aryl region whereas that at 170 ppm due to the C═O group remains intact, which refers to the ring-opening of the spirolactam conformation in presence of water molecules.

3 exhibits a weak absorption transition at ~550 nm(A_{550}) in basic medium (pH 9.2) with low molar extinction coefficient whereas it absorbs strongly in neutral pH or acidic medium (pH 4.0). The ~18 fold enhancement in absorption($A_{4.0pH}/A_{9.2pH}$) of **3** as a function of pH (Fig. 3a) is in accordance with the colour change and could be observed through the naked eye as the colour of the solution is faint pink in basic pH in contrast to the deep pink in acidic and neutral pH. The addition of trifluoroacetic acid (H^+) to the μM solution of **3** in MeCN/THF leads to an enhancement of the A_{550} absorption peak intensity [$\varepsilon_{(3.H+)}/\varepsilon_3$ = 192 (MeCN) and 505 (THF) fold] with concomitant color change from colorless to pink indicating delactonization of the spiro-ring in the presence of protons, which is in accordance with that observed in few rhodamine based probes[6i,n] reported earlier. This ascertains that the enhancement of A_{550} absorption of **3** in the presence of water molecules is due to water induced delactonization of the attached rhodamine. The reference compound **4**, which incorporates a *m*-xylyl- π-system in its architecture in comparison to the diethyl-amino-NBD segment of **3**, fails to respond towards water induced modulation of A_{550} absorption intensity under similar conditions. This infers that the central donor N-atom of **3** to which the NBD moiety is attached plays a crucial role in its water-induced spiro-ring opening and results in subsequent absorption amplification. Further, it has been observed that the μM solution of **3** in MeCN or THF also exhibits similar enhancement (Fig. 3b) in absorption in the presence of MeOH and EtOH as seen in case with H_2O, however, the extent of enhancement in the A_{550} absorption in the presence of 50% v/v MeOH or EtOH is much lower than that in the presence of 2% v/v H_2O. This infers that their 50% v/v concentration threshold for optimal absorption enhancement in comparison to a much lower concentration (2% v/v) for that of H_2O facilitates **3** to be a potential sensing system for H_2O molecules.

Emission in the presence of water

The addition of a trace amount of water to a sub-μM solution of **3** in THF, MeCN, acetone, DMF and DMSO significantly modulates its emission properties, leading to enhancement of fluorescence at ~580 nm (Fig. 4a) upon excitation at 450 nm. Addition of water not only perturbs the operative processes due to effective stabilization of excited ICT states but is also responsible for guest-bound ring opening of the spiro-cyclic structure; as a result, excitation of NBD at 350–450 nm region triggers a fluorescence resonance energy transfer (FRET) from excited NBD to ring-opened-amide-structured rhodamine which strongly fluoresces (λ_{em} = 580 nm). Fluorescence titration of **3** (3×10^{-8} M, MeCN, λ_{ex} = 350 nm) with water reveals that the intensity of the emission maxima (I/Io) enhances gradually up to addition of 2% v/v H_2O (1.11 mol L^{-1}) and further addition leads to a decrease in its fluorescence. Among all the solvents under investigation, the extent of optimal water induced fluorescence recovery in **3**

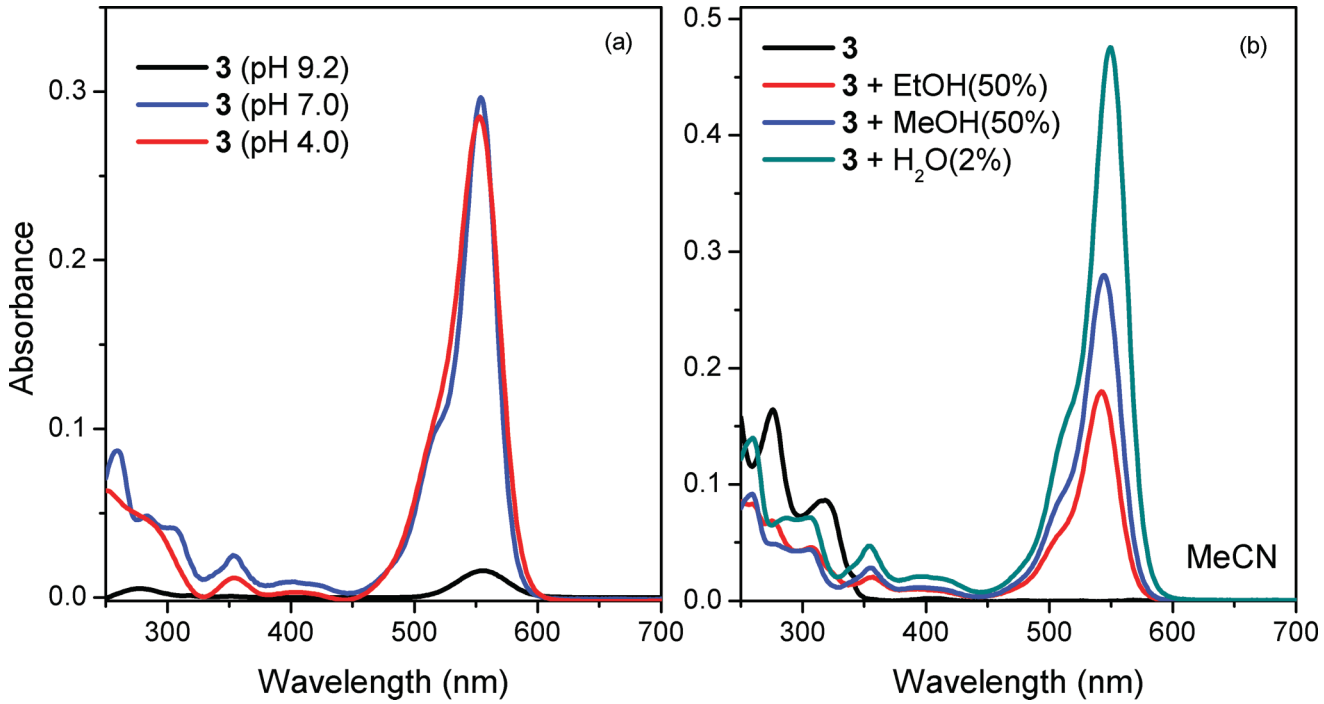

Fig. 3 (a) Absorption spectra of **3** in pH 4.0, 7.0 and 9.2 (conc. = 1×10^{-6} M). (b) Comparative absorption spectra of **3** in presence of EtOH (50% v/v), MeOH (50% v/v), H_2O (2% v/v) in MeCN (conc. = 1×10^{-6} M).

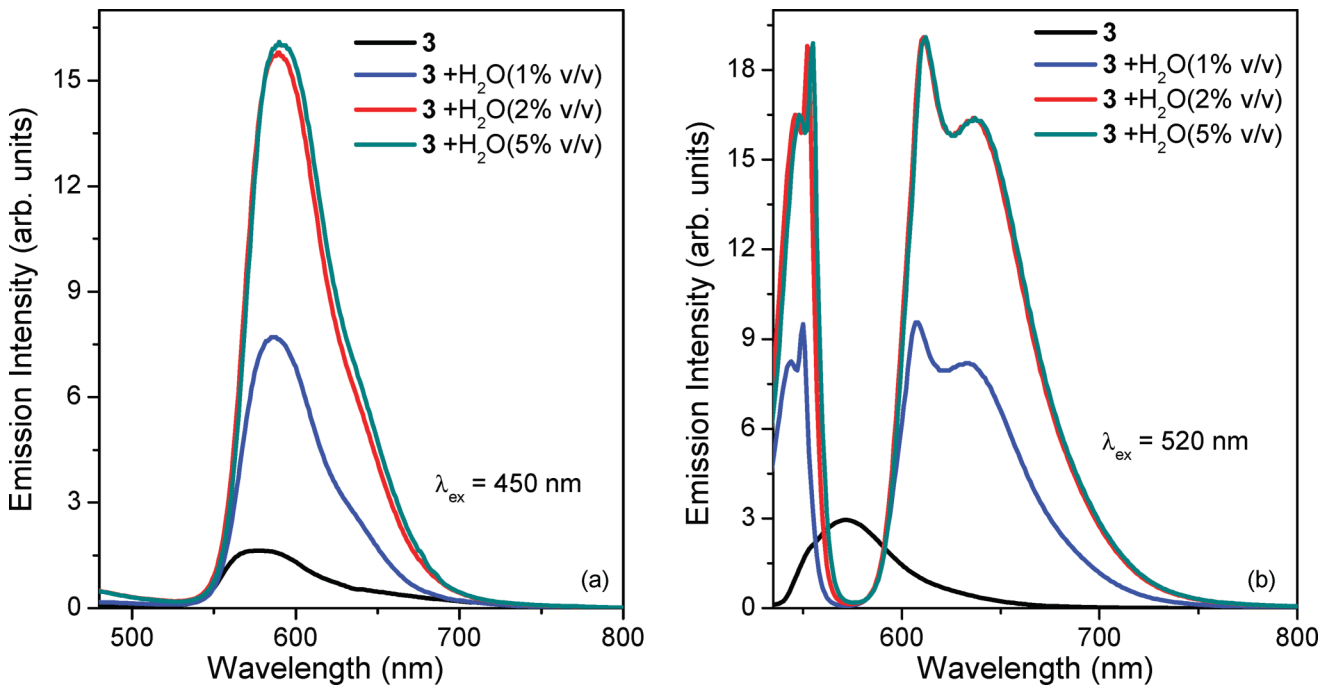

Fig. 4 Emission spectra of **3** alone and in the presence of H_2O (1%, 2% and 5% v/v) upon excitation at (a) λ_{ex} = 450 nm (b) λ_{ex} = 520 nm in MeCN at 1×10^{-6} M concentration. (The fluorescence intensities are scaled down to a factor of 10^6 for clarity).

could be observed in MeCN (~80 fold) with a detection limit of 0.1% v/v of water added at its 1×10^{-8} M concentration. The enhancement factor in fluorescence may not be as high as that in the case of absorption, yet increases to an appreciable fold (Table 1) in all the cases. On the contrary, addition of water to a solution of **2** and **4** in similar proportion leads to an expected further quenching of fluorescence, as it does in the case of **1**. Further, excitation of **3** at 520 nm in MeCN *i. e.* the wavelength where the nitrobenzofurazan moiety fluoresces to facilitate a FRET to the rhodamine, exhibits a quenched emission centered at 580 nm concomitant with that excited at 450 nm. However, the presence of H_2O leads to fluorescence enhancement with appearance of

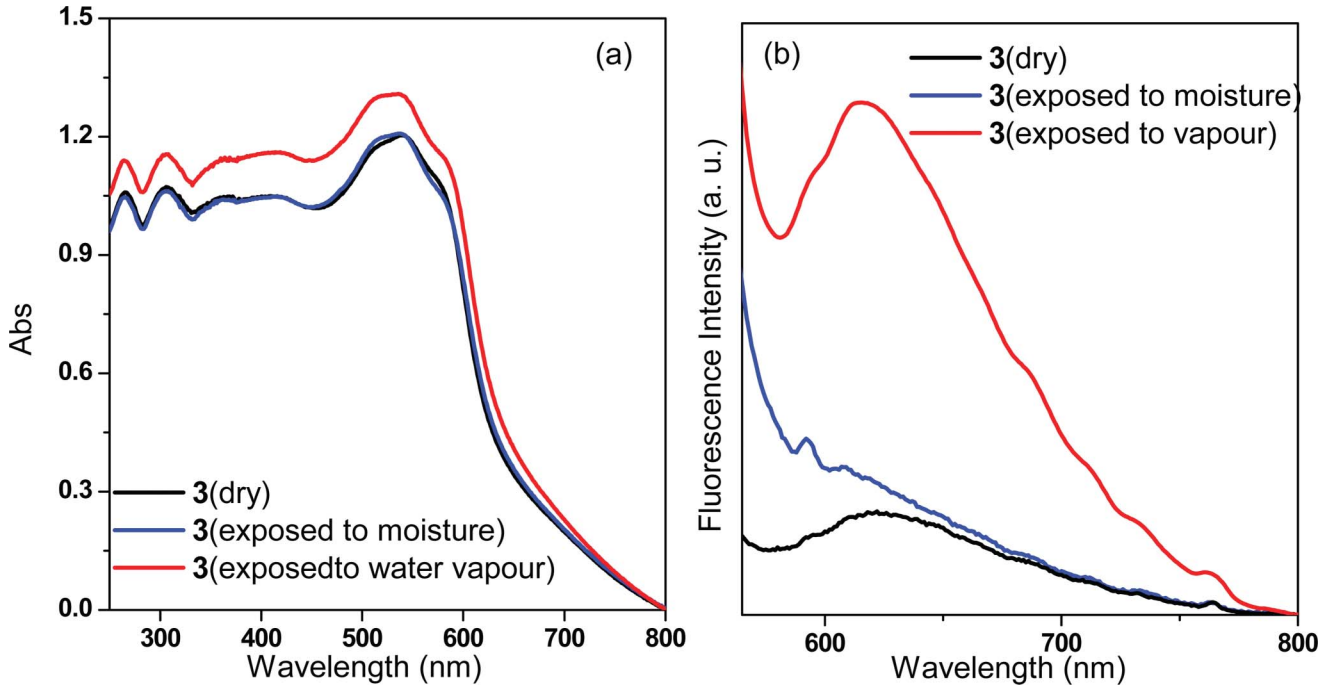

Fig. 5 Solid state absorption (a) and fluorescence (b) spectral pattern of **3** alone and in the presence of water under various conditions.

two new peaks at 550 nm and 620 nm (Fig. 4b). The excitation spectra monitoring both the (0,0) band of the structured emission (at 550 nm) and the λ_{max} of broad emission at 620 nm are found to be identical and match well with the absorption spectra of **3** in the solvents under investigation; this overrules formation of any ground state complexes among the fluorophores, and rather refers to an excited state event. Further, this higher wavelength emission is found to be insensitive towards solvent polarity and disappears in lower concentration of the solution ascertaining it to be due to an intramolecular excimer formation in **3** upon addition of water, not due to any exciplex formation. Hence, modulation of the emission pattern is due to a structural re-orientation in **3** in the presence of water molecules; the water-induced enhanced emission peak at 550 nm is attributable to that of ring-opened rhodamine whereas that at 620 nm refers to an excimer formation.

The reference molecule **1** in MeCN/THF exhibits fluorescence enhancement in the presence of protons through proton-induced inhibition[18,19] of operative PET process. Addition of trifluoroacetic acid (H^+) to **3** in MeCN/THF also leads to fluorescence enhancement at longer wavelength region [$(I^{(3.H+)}/I^3)_{em} \approx 66$ (MeCN) and 44 (THF) fold], which infers to the PET inhibition through protonation of donor amino-group, as a result, excitation of nitrobenzofurazan fluorophore induces a fluorescence resonance energy transfer (FRET) process to the proton-induced ring opened rhodamine which exhibits its fluorescence enhancement. The semi-empirical calculations for **3** and its proton mediated ring-opened structure reveal that the HOMO–LUMO energy gap of the rhodamine energy acceptor is higher than that of the NBD energy donor in guest free condition where the rhodamine exists in its spiro-lactam state and suppresses the energy transfer from excited NBD moiety to lactonized rhodamine. In presence of a guest, the spiro-ring of rhodamine delactonizes and hence the HOMO–LUMO energy gap of the ring-opened rhodamine lowers to match with that of excited NDB donor to facilitate the FRET process. Correlation with a similar spectral observation of **3** in the presence of water infers that the water molecules induce simultaneous perturbation of various photophysical processes such as (a) inhibition of operative PET from amino N-atom to excited NBD moiety, (b) inhibition of secondary PET to rhodamine, (c) opening of spiro-ring of rhodamine and (d) a subsequent initiation of the FRET process. Further, the absorption and emission maxima of the solvatochromic CT-transition of **3** do not vary much upon addition of 1–5% v/v H_2O to a MeCN or THF solution, contrary to that observed in **2**, which overrules the presumption that the water induced enhancement in absorption (colour change) and emission pattern could be due to change in solvent polarity upon addition of water. Thus, the probe **3** exhibits a simultaneous dual channel signaling in the presence of trace amounts of water with a detection limit of 0.3% v/v water added to its 1×10^{-6}M solution in MeCN for naked eye detection whereas that of 0.1% v/v of water added at 1×10^{-8}M concentration for fluorescence signal modulation.

Solid-state measurements

The effect of water molecules on the absorption and emission pattern of **3** in solid state follows that in the solution. **3** absorbs strongly at 540 nm in the dry state, remains unchanged upon overnight exposure to moisture, however, exhibits an enhanced and blue-shifted absorption peak at 529 nm upon exposure to water vapor/steam (Fig. 5a). Similarly, its weak emission at ~620 nm in dry conditions enhances to a small extent upon overnight exposure to moisture and fluoresces strongly upon exposure to water vapor (Fig. 5b). The spectral signaling pattern in the solid state is reversible as the enhanced fluorescence and absorption instantly disappears upon drying under reduced pressure and heat, retaining its initial spectral transition pattern.

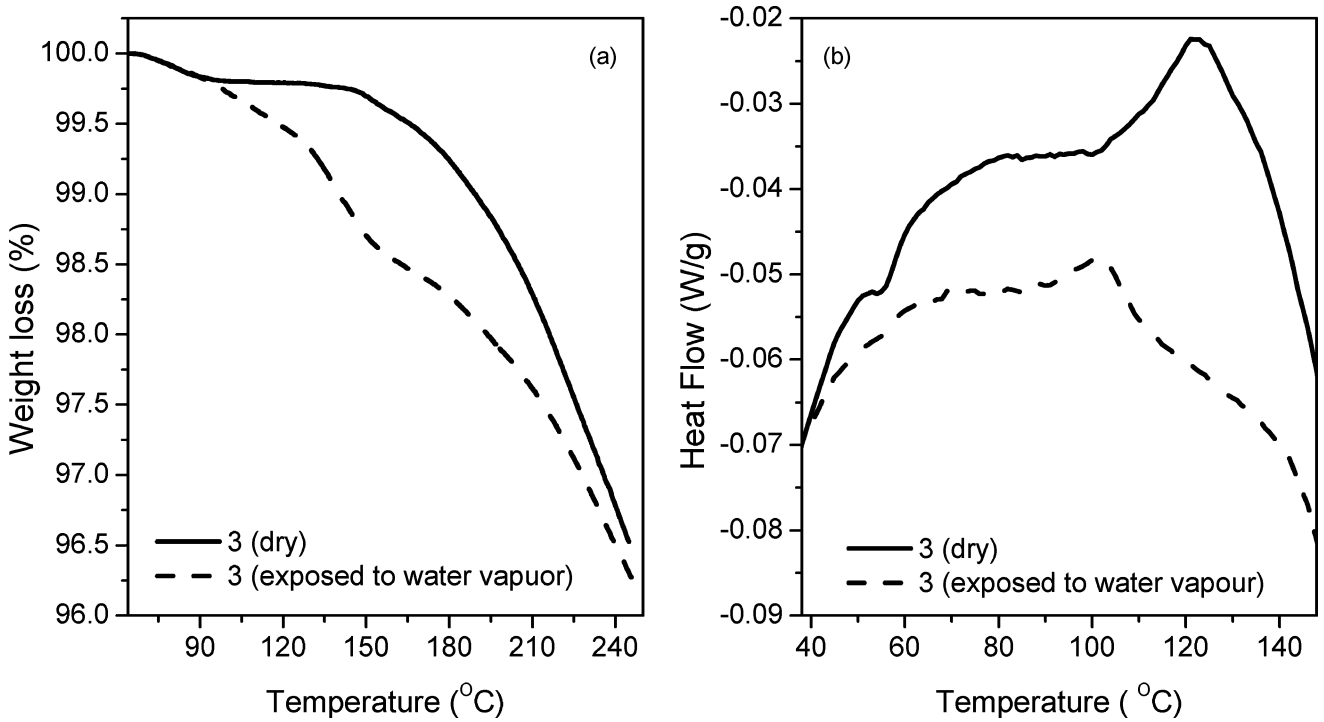

Fig. 6 TGA (a) and DSC (b) spectral patterns of **3** in dry and exposed to water vapour conditions.

The thermogravimetric analysis and differential scanning calorimetry studies of **3** both in dry and exposed to moisture conditions provide a qualitative correlation towards its solid state absorption and emission in the presence of water molecules. The probe **3** when exposed to water vapour results in a sharp slope in weight loss (%) at 122 °C in comparison to that in its dry condition (Fig. 6a); this is attributed to the loss of hydrogen-bonded water molecules within the receptor architecture. The DSC analysis (Fig. 6b) reveals that **3** undergoes a phase transition at 102 °C when exposed to water vapour in comparison to that at 121 °C in its dry condition. Further, **3** requires a higher (28.22 J g^{-1}) energy in its dry state to undergo the phase transition while that to be significantly lower (7.99 J g^{-1}) upon exposure to water vapour, which infers the presence of water molecules in the receptor framework attached through H-bonding. Though qualitative, the TGA and DSC analyses provide a structural basis towards interaction of water molecules with the probe molecule. Both the absorption and fluorescence data in both the solution and solid states leads to a water induced OFF–ON signaling situation in **3**, which further can be exploited as a moisture sensory devices. Emphasis on its structural pattern would have contributed beneficially to understand these properties through structure–function correlation before a conclusion can be put forward regarding its coordination environment; however, all attempts to obtain X-ray quality crystals of the **3** with H_2O remained unsuccessful.

Conclusion

In conclusion, a new amino receptor based signaling system **3**, designed and synthesized through a simple synthetic route with attached nitrobenzofurazan and rhodamine-B moieties in its architecture, acts as both fluorogenic and chromogenic chemosensor for water with high sensitivity by exploiting its spectroscopic properties. Addition of water to **3** in trace amounts leads to a prominent enhancement in absorption which could be used for naked-eye detection. The colour of its solutions in organic solvents such as MeCN, THF, acetone, DMF, and DMSO *etc.* changes in the presence of water with as low as 2% v/v concentration. It responds similarly in the presence of MeOH and EtOH, however, the optimal enhancement with 50% v/v MeOH or EtOH in organic solvents is much lower than that in the presence of water with 2% v/v concentration, a threshold that brings about its specificity towards water molecules. The water acts as a guest here rather than a medium to **3**. It also triggers a fluorescence resonance energy transfer process to facilitate enhancement in fluorescence in a longer wavelength region. The presence of water molecules not only suppresses the PET through H-bonding interactions but also facilitates the ring opening of rhodamine's spiro-lactam ring to initiate a FRET between the fluorophores. H-bonding interactions of water with the receptor plays a greater role in structural modification of **3** that reflects in the signal modulation. The solvent polarity plays a lesser role in chromogenic and fluorogenic sensing of water by **3** as the related compounds **1**, **2** and **4** do not exhibit similar signaling responses in the presence of water, even at higher concentration threshold. Its absorption and fluorescence spectral behavior in the solid state is concomitant with that in solution. Hence, the signal modulation in **3** in the presence of water molecules has the potential to be exploited as a moisture sensor and can find many futuristic material based applications upon suitable modification. Furthermore, its architecture as a receptor in association with substrate-induced spirolactam-ring opening transition has the potential to be exploited as a chemosensor for metal ions. We are presently working along these lines.

Materials and methods

All the reagent grade chemicals were used without purification unless otherwise specified. Bis-(2-chloroethyl)-ammonium chloride, 7-chloro-4-nitrobenz-2-oxa-1,3-diazole (7-chloro-4-nitrobenzofurazan), rhodamine-B hydrochloride, ethylenediamine, and the metal-perchlorate salts were obtained from Aldrich (U.S.) and used as received. Anhydrous potassium carbonate, acids, buffers and the solvents were received from S. D. Fine Chemicals (India). All the solvents were freshly distilled prior to use for fluorescence measurements by following the literature procedures and all the reactions were carried out under a N_2 atmosphere. Chromatographic separation were done by column chromatography using 100–200 mesh silica gel or neutral alumina.

The compounds were characterized by elemental analyses, ^{1}H-NMR, ^{13}C-NMR and mass (ESI) spectroscopy. ^{1}H-NMR and ^{13}C-NMR spectra were recorded on a JEOL JNM-AL400 FT V4.0 AL 400 (400 MHz and 100 MHz respectively) instrument in $CDCl_3$ with Me_4Si as the internal standard. Electrospray mass spectral data were recorded on a MICROMASS QUATTRO II triple quadruple mass spectrometer. The dissolved samples of the compounds in suitable solvents were introduced into the ESI source through a syringe pump at the rate of 5 μL min^{-1}, ESI capillary was set at 3.5 kV with 40V cone voltage and the spectra were recorded at 6 s scans. Melting points were determined with a melting point apparatus by PERFIT, India and were uncorrected. Elemental analyses were done in an Elementar Vario EL III Carlo Erba 1108 elemental analyzer. UV–visible spectra were recorded on a Perkin Elmer Lambda 650 UV/VIS spectrophotometer at 298 K in 10^{-4}–10^{-6} M concentration. Steady-state fluorescence spectra and solid state emission were obtained with a Fluoromax 4P spectrofluorometer at 298 K. Fluorescence quantum yield was determined in each case by comparing the corrected spectrum with that of Rhodamine G ($\phi_F = 0.95$) in EtOH[23] by taking the area under the total emission using the following the equation[24]

$$\phi_S = \phi_R\,(F_S A_R / F_R A_S)\cdot(\eta_S/\eta_R)^2 \qquad (1)$$

where ϕ_S and ϕ_R are the radiative quantum yields, F_S and F_R are the area under the fluorescence spectra, A_S and A_R are the absorbances (at the excited wavelength) of the respective sample and the reference; η_S and η_R are the refractive indices of the solvent used for the sample and the reference. The quantum yield of Rhodamine G was measured using quinine sulfate in 1 N H_2SO_4 as reference[25] at λ_{ex} of 350 nm. The standard quantum yield value thus obtained was used for the calculation of the quantum yield of the samples. The solid-state emission spectra were recorded with excitation at 350 nm with 450 W Xenon lamp, band pass 2 nm and slapped through 1 nm while recording the spectra, integration time was 0.2 s. Thermo-gravimetric analyses were carried out in a METTLER TG-DTA 851^E analyzer under a N_2 atmosphere within 60–250 °C temperature range with a scan rate of 5 °C min^{-1}. Differential scanning calorimetric analyses were carried out in a DSC Q20/TA analyzer with a heating rate of 0.5 °C min^{-1} within ambient to 150 °C temperature range under a N_2 atmosphere and ASTM D 3418 standard.

The structures of the compounds were geometrically optimized by employing the semi-empirical methods with convergence gradient <0.0001 in Hyperchem software.[26] The PM3 semi-empirical method was employed to calculate the change in dipole moments, minimal energy for these systems, nature of electronic transitions and their corresponding energies.

Synthesis

The compounds were synthesized as per the Scheme 1.

Synthesis of 7-[bis-(2-chloroethyl)-amino-nitro-benzofurazan, 1

To a stirring solution of bis-(2-chloro-ethyl)-ammonium chloride (0.2048 g, 1 mmol) in toluene (100 mL), K_2CO_3 (0.3 g, 2 mmol) was added followed by 7-chloro-4-nitro-benzofurazan (0.2033 g, 1 mmol). It was heated to reflux for 6 h with constant stirring, allowed to cool to room temperature and finally kept overnight at ice temperature. Solids were removed by filtration and the filtrate was evaporated under reduced pressure to obtain a brown solid. The desired product **1** was purified and isolated by column chromatography with silica gel (100–200 mesh) using 3% chloroform in hexane as eluent. Yield: 0.119 g (39%); mixed mp: 85 °C; ESI-MS, m/z^+ (%): 306 $[M+1]^+$, (30%); ^{1}H-NMR (400 MHz, $CDCl_3$, 25 °C TMS, δ): 3.44 (s, 2H, CH_2) 3.80 (s, 2H, CH_2), 3.98 (s, 2H, CH_2), 4.34 (s, 2H, CH_2) 7.61 (d, J = 8 Hz, 1H, Ar) 8.42 (d, J = 8 Hz, 1H, Ar), ^{13}C-NMR (100 MHz, $CDCl_3$, 25 °C, TMS, δ):149.46, 144.49, 143.63, 142.87, 134.77, 131.29, 130.48, 128.52, 102.39, 55.78, 49.22, 40.34, 38.48. Anal. Calcd. for $C_{10}H_{10}N_4O_3Cl_2$: C, 39.34, H, 3.30, N, 18.30. Found: C, 39.15; H, 3.49; N, 18.44%.

Synthesis of aminoethyl rhodamine, 2

This compound was synthesized following literature procedures.[7a–b] Yield: 80%; ESI-MS, m/z^+ (%): 485 $[M+1]^+$ (100%); ^{1}H-NMR (400 MHz, $CDCl_3$, 25 °C TMS, δ): 7.90(br s, 1H), 7.41(br s, 2H), 7.09(br s, 1H), 6.42(d, 2H, J = 7.99 Hz), 6.37(s, 2H), 6.26(d, 2H, J = 7.99 Hz), 3.32(d, 8H, J = 7.99 Hz), 3.19(s, 2H), 2.41(br s, 2H), 1.15(t, 12H, J = 7.99 Hz); ^{13}C-NMR (100 MHz, $CDCl_3$, 25 °C, TMS, δ):168.47, 153.26(d), 148.63, 132.27, 131.13, 128.66(d), 127.91, 123.70, 122.61, 107.95(d), 105.49(d), 97.67(d), 64.49, 44.22, 43.76, 40.70, 30.81. 12.47; Anal. Calcd. for $C_{30}H_{36}N_4O_2$: C, 74.35, H, 7.49, N, 11.56. Found: C, 74.19; H, 7.63; N, 11.41%.

Synthesis of 3

To a stirring ethanolic solution of **1** (0.5 g, 1.64 mmol), K_2CO_3(0.552 g, 4.0 mmol) was added followed by drop-wise addition of ethylene diamine (0.3 mL, 4.48 mmol) in ethanol (10 mL) and heated to reflux for 24 h with constant stirring. The reaction mixture was filtered while hot and the solvent was evaporated to dryness. The residual semi-solid was washed with water (3 × 50 mL) and extracted with $CHCl_3$. The organic layer, after drying over Na_2SO_4, was evaporated under reduced pressure to get a reddish-brown foamy solid, **1a** (Yield: 78%). To an ethanolic solution of **1a** (0.81 g, 2.3 mmol), rhodamine B (2.25 g, 4.7 mmol) dissolved in ethanol was added drop-wise over a period of 3 h with vigorous stirring at room temperature and the reaction mixture was heated to reflux for 20 h until the colour of the solution changes from pink to orange. The solvent was then evaporated to dryness to result in an orange residual mass. Water (20 mL) was added to it and extracted with CH_2Cl_2 (30 mL × 3). The combined organic phase was dried over Na_2SO_4 and the solvent was removed

by evaporation under reduced pressure to afford a dark orange solid of **3**. It was further purified by passing through a column (neutral alumina) with chloroform and methanol mixture (98 : 2 v/v). Yield: 1.96 g (71%); mixed mp: 158–160 °C; ESI-MS, m/z^+ (%): 1218 $[M+H_2O]^+$, (39%); ^{1}H-NMR (400 MHz, $CDCl_3$, 25 °C, TMS, δ): 8.01 (d, J = 7.99 Hz, 2H), 7.63 (q, J = 7.99 Hz, 3H), 7.22 (d, J = 7.99 Hz, 3H), 6.58 (d, J = 7.99 Hz, 8H), 6.43 (d, J = 3.99 Hz, 4H), 6.34 (dd, J = 7.99 Hz, 2H), 3.35 (dd, J = 7.99 Hz, J = 3.99 Hz, 32H), 1.15 (t, J = 7.99 Hz, 24H); ^{13}C-NMR (100 MHz, $CDCl_3$, 25 °C, TMS, δ):169.91, 153.46, 152.07, 149.63, 134.11, 129.12, 129.02, 128.41, 124.90, 124.31, 108.14, 106.19, 97.42, 65.76, 44.45, 40.86, 12.47; Anal. Calcd. for $C_{70}H_{80}N_{12}O_7$: C, 69.98, H, 6.71, N, 13.99. Found: C, 69.44; H, 6.87; N 13.63%.

Synthesis of 4

To a stirring ethanolic solution (80 mL) of **2** (3.03 g, 6.25 mmol), isophthalaldehyde (0.416 g, 3.1 mmol) was added and allowed to stir for 24 h at room temperature till the solution became turbid. The Schiff-base imine thus formed was reduced with $NaBH_4$, and was further refluxed for 2 h to ensure the complete reduction (the solution became transparent). The solvent was evaporated to dryness under reduced pressure. Water (50 mL) was added to the residual mass and extracted with $CHCl_3$ (3 × 30 mL). The combined organic layers were dried over Na_2SO_4, filtered and evaporated to dryness to obtain a pale orange solid. It was further purified by passing through a column (100–200 mesh silica gel) with chloroform and methanol mixture (98 : 2 v/v). Yield: 2.83 g (85%); mixed mp: 168–170 °C; ESI-MS, m/z^+ (%): 1071 $[M]^+$, (42%); ^{1}H-NMR (300 MHz, $CDCl_3$, 25 °C, TMS, δ):7.88 (s, 2H), 7.42 (dd, J = 3.301 Hz, 4H), 7.18 (t, J = 7.503 Hz, 1H), 7.02 (m, 4H), 6.42 (s, 2H), 6.39 (s, 1H), 6.36 (d, J = 2.10 Hz, 8H), 6.25 (d, J = 2.40 Hz, 1H), 6.22 (d, J = 2.1 Hz, 1H), 4.60 (s, 4H), 3.59 (s, 16H), 3.31 (t, J = 6.61 Hz, 4H), 2.39 (t, J = 6.30 Hz, 4H), 1.133 (t, J = 6.90 Hz, 24H); ^{13}C-NMR (100 MHz, $CDCl_3$, 25 °C, TMS, δ): 167.24, 157.09, 142.22, 142.5, 136.82, 134.88, 131.04, 128.98, 128.32, 128.02, 127.36, 126.62, 125.76, 121.49, 106.7, 103.66, 65.03, 48.62, 48.46, 44.34, 41.79, 15.2, 12.84; Anal. Calcd. for $C_{68}H_{78}N_8O_4$: C, 76.23, H, 7.34, N, 10.46. Found: C, 76.04; H, 7.48; N, 10.29%.

Acknowledgements

BPB wishes to thank Department of Science and Technology, New Delhi for the financial support (SR/FTP/CS-138/2006) for this work. The authors sincerely wish to thank the Director, IMMT for a CSIR-diamond jubilee research internship to AP.

References

1 For reviews, see: (*a*) J. S. Kim and D. T. Quang, *Chem. Rev.*, 2007, **107**, 3780; (*b*) B. Bag and P. K. Bharadwaj, *Photo, Electrochemistry & Photobiology in the Environment, Energy and Fuel*, S. Kaneco ed., 2007, **201**; (*c*) V. Amendola, L. Fabbrizzi, F. Forti, M. Licchelli, C. Mangano, P. Pallavicini, A. Poggi, D. Sacchi and A. Taglieti, *Coord. Chem. Rev.*, 2006, **250**, 273; (*d*) J. F. Callan, A. P. de Silva and D. C. Magri, *Tetrahedron*, 2005, **61**, 8551; (*e*) A. P. de Silva, H. Q. N. Gunaratne, T. Gunnlauggsson, A. J. M. Huxley, C. P. McCoy, J. T. Radmacher and T. E. Rice, *Chem. Rev.*, 1997, **97**, 1515.

2 (*a*) M. Santra, D. Ryu, A. Chaterjee, S. K. Ko, I Shin and K. H. Ahn, *Chem. Commun.*, 2009, 2115; (*b*) L. D. Lavis and R. T. Raines, *ACS Chem. Biol.*, 2008, **3**, 142; (*c*) L. D. Lavis, T.-Y. Chao and R. T. Raines, *ACS Chem. Biol.*, 2006, **1**, 252; (*d*) M. R. Longmire, M. Ogawa, Y. Hama, N. Kosaba, C. A. S. Regino, P. L. Choyke and H. Kobayashi, *Bioconjugate Chem.*, 2008, **19**, 1735; (*e*) B. Tang, Y. Xiang, P. Li, N. Zhang, F. Yu and G. Yang, *J. Am. Chem. Soc.*, 2007, **129**, 11666; (*f*) S. Kumar, B. Zhou, F. Liang, H. Yang, W.-Q. Wang and Z.-Y. Zhang, *J. Proteome Res.*, 2006, **5**, 1898.

3 (*a*) V. Tsyalkovsky, V. Klep, K. Ramaratnam, R. Lupitskyy, S. Minko and I. Luzinov, *Chem. Mater.*, 2008, **20**, 317; (*b*) Y.-R. Kim, H. J. Kim, J. S. Kim and H. Kim, *Adv. Mater.*, 2008, **20**, 4428; (*c*) S. Wu, Y. Luo, F. Zeng, J. Chen, Y. Chen and Z. Tong, *Angew. Chem., Int. Ed.*, 2007, **46**, 6933; (*d*) L. Shi, V. D. Paoli, N. Rosenzweig and Z. Rosenzweig, *J. Am. Chem. Soc.*, 2006, **128**, 10378; (*e*) F. D. Monte, J. D. Mackenzie and D. Levy, *Langmuir*, 2000, **16**, 7377.

4 H. N. Kim, M. H. Lee, H. J. Kim, J. S. Kim and J. Yoon, *Chem. Soc. Rev.*, 2008, **37**, 1465.

5 Recent examples of rhodamine based probes for transition and heavy metal ions: (*a*) H. Li, J. Fan, J. Du, K. Guo, S. Sun, X. Liu and X. Peng, *Chem. Commun.*, 2010, **46**, 1079; (*b*) W. Shi, S. Sun, X. Li and H. Ma, *Inorg. Chem.*, 2010, **49**, 1206; (*c*) Y. Zhao, Y. Sun, X. Lv, Y. Liu, M. Chen and W. Guo, *Org. Biomol. Chem.*, 2010, **8**, 4143; (*d*) W. Lin, L. Long, B. Chen, W. Tan and W. Gao, *Chem. Commun.*, 2010, **46**, 1311; (*e*) Z. Q. Hu, C. S. Lin, X. M. Wang, L. Ding, C.-L. Cui, S.-F. Liu and H. Y. Lu, *Chem. Commun.*, 2010, **46**, 3765; (*f*) W. Lin, X. Cao, Y. Ding, L. Yuan and L. Long, *Chem. Commun.*, 2010, **46**, 3529; (*g*) J. Mao, Q. He and W. Liu, *Talanta*, 2010, **80**, 2093.

6 Some more examples of rhodamine based probes for metal ions: (*a*) G. He, D. Guo, C. He, X. Zhang, X. Zhao and C. Duan, *Angew. Chem., Int. Ed.*, 2009, **48**, 6132; (*b*) J. Huang, Y. Xu and X. Qian, *J. Org. Chem.*, 2009, **74**, 2167; (*c*) Y. K. Yang, S. Lee and J. Tae, *Org. Lett.*, 2009, **11**, 5610; (*d*) M. Suresh, S. Mishra, S. K. Mishra, E. Suresh, A. K. Mandal, A. Shrivastav and A. Das, *Org. Lett.*, 2009, **11**, 2740; (*e*) Y. Zhao, X.-B. Zhang, Z.-X. Han, L. Qiao, C.-Y. Li, L.-X. Jian, G.-L. Shen and R.-Q. Yu, *Anal. Chem.*, 2009, **81**, 7022; (*f*) L. Zhang, J. Fan and X. Peng, *Spectrochim. Acta, Part A*, 2009, **73**, 398; (*g*) Y.-K. Yang, S. Lee and J. Tae, *Org. Lett.*, 2009, **11**, 5610; (*h*) W. Shi and H. Ma, *Chem. Commun.*, 2008, 1856; (*i*) X. Q. Zhan, Z. H. Qian, H. Zheng, B.-Y. Su, Z. Lan and J.-G. Xu, *Chem. Commun.*, 2008, 1859; (*j*) J.-S. Wu, I.-C. Hwang, K. S. Kim and J. S. Kim, *Org. Lett.*, 2007, **9**, 907; (*k*) H. Yang, Z. Zhou, K. Huang, M. Yu, F. Li, T. Yi and C. Huang, *Org. Lett.*, 2007, **9**, 4729; (*l*) Y. Xiang and A. Tong, *Org. Lett.*, 2006, **8**, 1549; (*m*) Y. Xiang, A. Tong, P. Jin and Y. Ju, *Org. Lett.*, 2006, **8**, 2863; (*n*) H. Zheng, J.-H. Qian, L. Xu, F.-F. Yuan, L.-D. Lan and J.-G. Xu, *Org. Lett.*, 2006, **8**, 859; (*o*) J. Y. Kwon, Y. J. Jang, Y. J. Lee, K. M. Kim, M. S. Seo, W. Nam and J. Yoon, *J. Am. Chem. Soc.*, 2005, **127**, 10107.

7 (*a*) X. Zhang, Y. Shiraishi and T. Hirai, *Org. Lett.*, 2007, **9**, 5039; (*b*) J. H. Soh, K. M. K. Swamy, S. K. Kim, S. Kim, S.-H. Lee and J. Yoon, *Tetrahedron Lett.*, 2007, **48**, 5966; (*c*) X. Zhang, Y. Shiraishi and T. Hirai, *Tetrahedron Lett.*, 2007, **48**, 5455; (*d*) Y.-K. Yang, K.-J. Yook and J. Tae, *J. Am. Chem. Soc.*, 2005, **127**, 16760; (*e*) V. Dujols, F. Ford and A. W. Czarnik, *J. Am. Chem. Soc.*, 1997, **119**, 7386.

8 C. Kaewtong, J. Noiseephum, Y. Uppa, N. Morakot, N. Morakot, B. Wanno, T. Tuntulani and B. Pulpoka, *New J. Chem.*, 2010, **34**, 1104.

9 X. Chen, X. Wang, S. Wang, W. Shi, K. Wang and H. Ma, *Chem.–Eur. J.*, 2008, **14**, 4719.

10 Y. K. Yan, H. J. Cho, J. Lee, I. Shin and J. Tae, *Org. Lett.*, 2009, **11**, 859.

11 (*a*) H. Zheng, G.-Q. Shang, S.-Y. Yang, X. Gao and J.-G. Xu, *Org. Lett.*, 2008, **10**, 2357; (*b*) T. Rieth and K. Sasamoto, *Anal. Commun.*, 1998, 195.

12 C. J. stephenson and K. D. Shimizu, *Org. Biomol. Chem.*, 2010, **8**, 1027.

13 X. Lou, L. Zhang, J. Kin and Z. Li, *Langmuir*, 2010, **26**, 1566.

14 F. Renz, P. A. De Souza, G. Kingelhöfer and H. A. Goodwin, *Hyperfine Interact.*, 2002, **193–140**, 699.

15 (*a*) T. Förster, *Z. Naturforsch.*, 1949, **49**, 321; (*b*) H. C. Cheung, in *Topics in Fluorescence Spectroscopy*, J. R. Lakowicz, ed., Plenum press, New York, 1991, **2**, 128; (*c*) K. E. Sapsford, L. Berti and I. L. Medintz, *Angew. Chem., Int. Ed.*, 2006, **45**, 4562; (*d*) K. K. Sadhu, B. Bag and P. K. Bharadwaj, *Inorg. Chem.*, 2007, **46**, 8051.

16 M. H. Lee, H. J. Kim, S. Yoon, N. Park and J. S. Kim, *Org. Lett.*, 2008, **10**, 213.

17 The synthesis of aminoethyl rhodamine **2** has been reported earlier, see references 7a–b; however, the absorption and emission spectroscopic properties in various solvents were not discussed elsewhere.

18 B. Bag and P. K. Bharadwaj, *Inorg. Chem.*, 2004, **43**, 4626.

19 S. Uchiyama, K. Takehira, S. Kohtani, K. Imai, R. Nakagaki, S. Tobita and T. Santa, *Org. Biomol. Chem.*, 2003, **1**, 1067.
20 The μM solution of **3** in MeOH and EtOH exhibits pink color with high molar extinction coefficient at ~550 nm attributed to the solvent assisted ring-opening of the spiro-structure.
21 B. Ramachandram and A. Samanta, *J. Phys. Chem. A*, 1998, **102**, 10579.
22 S. F. Forgues, J. P. Fayet and A. Lopez, *J. Photochem. Photobiol., A*, 1993, **70**, 229.
23 M. Fischer and J. Georges, *Chem. Phys. Lett.*, 1996, **260**, 115.
24 (*a*) B. Bag and P. K. Bharadwaj, *J. Phys. Chem. B*, 2005, **109**, 4377; (*b*) S. Uchiyama, Y. Matsumura, A. P. de Silva and K. Iwai, *Anal. Chem.*, 2003, **75**, 5926.
25 J. B. Birks, *Photophysics of Aromatic Molecules*, Wiley-Interscience, New York, 1970.
26 HyperChem®Release 7 for Windows®, HyperCube, Inc.: Gainesville, FL, 2002.